Journal of Inflammation Research

Dovepress
Taylor & Francis Group

Open Access Full Text Article

ORIGINAL RESEARCH

Inflammatory Gene Signature Identified by Machine Algorithms Reveals Novel Biomarkers of Coronary Artery Disease

Xing Liu[1,*], Yuanyuan Zhang[1,*], Yan Wang[2,3,*], Yanfeng Xu[2,4,5], Wenhao Xia[2,5–7], Ruiming Liu[4,5], Shiyue Xu[2,5,6]

[1]Department of Cardiology, The Third Affiliated Hospital, Sun Yat-sen University, Guangzhou, Guangdong, People's Republic of China; [2]Department of Hypertension and Vascular Disease, The First Affiliated Hospital, Sun Yat-sen University, Guangzhou, Guangdong, People's Republic of China; [3]Health Management Center, The First Affiliated Hospital, Sun Yat-sen University, Guangzhou, Guangdong, People's Republic of China; [4]Laboratory of General Surgery, The First Affiliated Hospital, Sun Yat-sen University, Guangzhou, Guangdong, People's Republic of China; [5]National - Guangdong Joint Engineering Laboratory for Diagnosis and Treatment of Vascular Diseases, Sun Yat-sen University, Guangzhou, Guangdong, People's Republic of China; [6]NHC Key Laboratory of Assisted Circulation, Sun Yat-sen University, Guangzhou, Guangdong, People's Republic of China; [7]Department of Cardiovascular Medicine, Guangxi Hospital Division of The First Affiliated Hospital of Sun Yat-sen University, Nanning, Guangxi, People's Republic of China

*These authors contributed equally to this work

Correspondence: Shiyue Xu, Department of Hypertension and Vascular Disease, The First Affiliated Hospital, Sun Yat-sen University, Guangzhou, 510080, People's Republic of China, Email xushy25@mail.sysu.edu.cn; Ruiming Liu, Laboratory of General Surgery, The First Affiliated Hospital, Sun Yat-sen University, Guangzhou, 510080, People's Republic of China, Email liuruim@mail2.sysu.edu.cn

Purpose: Inflammatory activation of immune cells plays a pivotal role in the development of coronary artery diseases (CAD). This study aims to investigate the immune responses of peripheral blood mononuclear cells (PBMCs) in CAD and to identify novel signature genes and biomarkers using machine learning algorithms.

Methods: The GSE113079 dataset was analyzed and differentially expressed genes (DEGs) were identified between CAD and normal samples. The intersection of DEGs with inflammation-related genes was used to identify the differentially expressed inflammation-related genes (DIRGs). Then, the receiver operating characteristic (ROC) curves were plotted for each DIRG, and those with an area under the curve (AUC) greater than 0.9 were selected for subsequent analysis. Furthermore, machine learning algorithms were employed to identify biomarkers. A nomogram was developed based on these biomarkers. The CIBERSORT algorithm and Wilcoxon test method were used to analyze the differences in immune cells between the CAD and normal samples. The identified biomarkers were validated in PBMCs from patients with CAD and in atherosclerotic aortas from $ApoE^{-/-}$ mice.

Results: A total of 574 DEGs were identified between CAD and normal samples. From this intersection, 29 DIRGs were identified, of which 14 DIRGs (*PTGER1*, *IL17RC*, *KLKB1*, *GPR32*, *ADM*, *NUPR1*, *SCN9A*, *IL17B*, *CX3CL1*, *FFAR3*, *PYDC2*, *SYT11*, *RORA*, and *GPR31*) exhibited high diagnostic efficacy. Four biomarkers (*ADM*, *NUPR1*, *PTGER1*, and *PYDC2*) were identified using Support Vector Machine (SVM). Ten types of immune cells, including $CD8^+$ T cells, regulatory T cells (Tregs), and resting NK cells, showed significant differences between the CAD and normal groups. Furthermore, increased levels of *ADM*, *NUPR1*, *PTGER1*, and *PYDC2* were validated in PBMCs isolated from CAD patients. In addition, *ADM*, *NUPR1*, and *PTGER1* were upregulated in the mouse atherosclerotic aorta.

Conclusion: Our findings revealed novel inflammatory gene signatures of CAD that could be potential biomarkers for the early diagnosis of CAD.

Keywords: inflammation, coronary artery disease, machine learning, immune infiltration

Introduction

Coronary artery disease (CAD) is the most common cause of mortality globally.[1,2] The pathogenesis of coronary artery disease is complex and asymptomatic in the early stages. Coronary angiography is the gold standard for the diagnosis of

Received: 30 October 2024
Accepted: 30 January 2025
Published: 10 February 2025

CAD; however, its high cost limits its widespread use, and approximately 39.2% of patients undergoing invasive coronary angiography exhibit less than 20% stenosis in the coronary artery.[3] Thus, it is important to identify reliable biomarkers for the early diagnosis of CAD and reduce invasive coronary angiography in patients with low coronary artery stenosis.

CAD is characterized by chronic inflammatory responses within the arterial walls that lead to atherosclerotic lesions and blockage of vessels.[4] Inflammation is a key driver of all the steps involved in atherosclerosis, including endothelial damage, activation of innate and adaptive immune responses, and recruitment of immune cells.[5] A growing number of studies have suggested that anti-inflammatory and immunomodulatory therapies targeting atherosclerosis and cardiovascular disease are promising.[6–9] However, the crosstalk between inflammation-related genes and the immune microenvironment in CAD remains unclear and warrants further investigation. Assessing and treating the residual inflammatory risk is expected to provide new directions for preventing CAD.

In recent years, comprehensive bioinformatics analysis and machine learning algorithms have led to the discovery of new genes associated with various diseases, which can serve as biomarkers for diagnosis and prognosis.[10] However, the diagnostic value of the genes associated with inflammatory activation in CAD remains unclear. Identifying effective inflammatory biomarkers is critical for the prevention and treatment of CAD. In the present study, we analyzed the GSE113079 dataset from various perspectives and developed an optimal diagnostic model for CAD using machine learning methods to identify inflammation-related genes that can serve as diagnostic markers for CAD. Further validation of the biomarkers was performed in patients with CAD and in a mouse atherosclerosis model. Our results provide a theoretical basis for the diagnosis of CAD and the identification of potential therapeutic targets.

Materials and Methods

Data Sources

A transcriptomic dataset of coronary artery disease (CAD) was obtained from the Gene Expression Omnibus (GEO) database (http://www.ncbi.nlm.nih.gov/geo/). The GSE113079 dataset comprised 48 normal and 93 CAD samples, all of which were peripheral blood samples. In addition, 910 inflammation-related genes were retrieved from the Molecular Signatures Database (MSigDB) Database (https://www.gsea-msigdb.org/gsea/msigdb/index.jsp).

Differential Expression Analysis and Enrichment Analysis

In this study, differentially expressed genes (DEGs) between CAD and normal samples in the GSE113079 dataset were acquired using the limma (v 3.46.0) package (p.value < 0.05, $|\log_2 FC| > 1$).[11] A heat map and volcano map of DEGs between CAD and normal samples were plotted using the pheatmap and ggplot2 packages,[12] respectively. Furthermore, DEGs between CAD and normal samples and inflammation-related genes were crossed to identify the differentially expressed inflammation-related genes (DIRGs). Subsequently, to better understand the related biological functions and signaling pathways involved in the above DIRGs, the Gene Ontology (GO), REACTOME, and Genomes (KEGG) enrichment analyses were performed using clusterProfiler (v 4.0.2) package (p.adj < 0.05, count ≥ 2).[13]

Construction of Diagnostic Model

Receiver operating characteristic (ROC) curves for each DIRGs were plotted to select genes with high diagnostic efficacy (area under the curve (AUC), > 0.9). In the GSE113079 dataset, we divided the samples into training and validation set according to 7:3. Subsequently, nine types of machine algorithms–K-Nearest Neighbor (KNN), Random Forest (RF), logistic regression (LR), Support Vector Machine (SVM), decision tree (DT), XGBoost, LightGBM, Artificial Neural Network (ANN), and CatBoost–were used in the training set to construct diagnostic models based on genes with high diagnostic efficacy. ROC curves of the nine models were plotted for the validation set. The model with the highest AUC value was selected as the final diagnostic model to identify biomarkers. In addition, principal component analysis (PCA) was performed based on the expression levels of biomarkers in GSE113079 dataset, and a coefficient diagram of the biomarkers was drawn.

Construction of Nomogram

Based on the biomarkers obtained from the above analysis, a nomogram for disease probability prediction in patients with CAD was created using the rms (v. 6.1–0) package. Moreover, calibration, decision, and clinical impact curves were analyzed to evaluate the precision of the prediction.

Gene Set Enrichment Analysis (GSEA)

To further explore the related signaling pathways and functional items associated with the biomarkers, we first calculated the correlation between the biomarkers and all other genes in the GSE113079 dataset. We then sorted all genes according to this correlation from high to low; GSEA was performed using the clusterProfiler (v 4.0.5) package.[13]

Immune Microenvironment Analysis

To study the infiltration of immune cells in the CAD and normal groups, the CIBERSORT algorithm and LM22 gene set were used to calculate the proportion of 22 immune cells. Furthermore, the Wilcoxon test was used to analyze whether there were differences in immune cells between CAD and normal samples ($p < 0.05$). Finally, we calculated the relationship between the biomarkers and all immune cells using the Pearson's method.

The Construction of miRNA-TF-mRNA Network

The miRNAs corresponding to the biomarkers were obtained from the miRWalk online database. The transcription factors (TFs) of the biomarkers were predicted using the AnimalTFDB online database. The regulatory relationship between TF and miRNAs was predicted using the TransmiR online tool. In addition, we used the miRWalk database to predict the regulatory relationships between miRNAs and TFs. Based on the reference,[14] we defined that if two miRNAs contained three or more co-regulated mRNAs, they were considered to have potential interaction possibilities. Finally, a miRNA-TF-mRNA network was created. To further analyze whether the network conformed to a scale-free network, we created a regression model using the connection degree as the independent variable and the number of nodes as the dependent variable, and then drew a topological feature map of the network. In addition, FANMOD software was utilized to draw the 3-node and 4-node network models of the above network. Additionally, we selected the network mode with a feedforward loop from the 3-node network mode, and the network mode with two feedforward loops from the 4-node network mode.

Subject Characteristics

Patients aged 18 years or older diagnosed with CAD by coronary computed tomography angiography or coronary angiography (stenosis ≥ 50% of the diameter of the major coronary arteries and their large branches) were enrolled in the CAD group (n=8, 6 males and 2 females, CAD group). Age-matched patients without CAD were enrolled in the control group (n=8; 6 males and 2 females, normal group). Patients with a history of malignancy, acute coronary syndrome, pulmonary embolism, or renal failure [glomerular filtration rate<60 mL/(min.1.73 m^2)] were excluded. The characteristics of the CAD and control groups are presented in Supplementary Table 1. This study was approved by the Institutional Review Board of the Third Affiliated Hospital of Sun Yat-sen University, which complies with the Declaration of Helsinki. Informed consent was obtained from all participants before participation in the study.

Animal Experiment

ApoE-deficient mice ($ApoE^{-/-}$) were obtained from GemPharmatech (Nanjing,China). All animal experiments received approval from the Institutional Animal Care and Use Committee of the First Affiliated Hospital of Sun Yat-sen University, adhering to the Guidelines for Ethical Review of Laboratory Animals—General Code of Animal Welfare (GB/T 42011–2022) issued by the Standardization Administration of China. $ApoE^{-/-}$ mice were fed a 45% high-fat diet (TP26303; Trophic Animal Feed High-tech Company, Nantong, China) or normal chow for eight weeks. After 8 weeks, the mice were anesthetized with 10% chloral hydrate, euthanized, and their tissues were collected.

Realtime-PCR

RNA from peripheral blood mononuclear cells (PBMCs) and mouse aorta was extracted using Nuclezol LS RNA Isolation Reagent (ABP Biosciences Inc.) according to the manufacturer's instructions. Total RNA was extracted using the TRIzol reagent (Invitrogen, Thermo Fisher, CA, USA) following the manufacturer's protocol. The extracted RNA was reverse-transcribed into cDNA using the RevertAid First Strand cDNA Synthesis Kit (Thermo Fisher Scientific). Reverse transcription was performed using a Transcript II real-time polymerase chain reaction (RT-qPCR) kit (Transgen, Beijing, China), followed by semi-quantitative RT-PCR using the Bio-Rad iQ5. Data were normalized to the mRNA levels of GADPH, which was used as a control gene, and analyzed using the $2^{-\Delta\Delta}$CT method. The detailed primer sequences are provided in Supplementary Table 2.

Statistical Analysis

All data were analyzed using the R software (version 4.0.0). The Two-sample *t*-test and Wilcoxon test were used to compare data between the two groups, and significant differences were considered at $p < 0.05$, unless specified otherwise.

Results

Acquisition of DEGs and DIRGs in CAD

A total of 574 DEGs were identified between CAD and normal samples (Figure 1A, Supplementary 3). The expression heatmap of the top 100 DEGs is shown in Figure 1B. Twenty-nine DIRGs were identified by intersecting DEGs with inflammation-related genes (Figure 1C). According to the GO functional enrichment analysis, DIRGs were involved in 264 GO items including 'regulation of inflammatory response', 'chemokine-mediated signaling pathway', 'response to chemokine' (Figure 1D, Supplementary 4). The KEGG functional enrichment analysis revealed that DIRGs were enriched in 24 KEGG pathways, including 'Cytokine-cytokine receptor interaction', 'Lipid and atherosclerosis', and "IL-17 signaling pathway" (Figure 1E, Supplementary 5). Furthermore, the REACTOME functional enrichment analysis demonstrated an association with 12 REACTOME pathways, including 'Chemokine receptors bind chemokines', "Interleukin-10 signaling", and "GPCR ligand binding" (Figure 1F, Supplementary 6). These enriched pathways represent key inflammatory mechanisms involved in the development of atherosclerosis.[15–17]

Biomarker Exploration and Diagnostic Model Construction by Machine Algorithms

We divided the GSE113079 dataset into training and validation sets in a 7:3 ratio. Based on an AUC greater than 0.9, 14 DIRGs (*PTGER1*, *IL17RC*, *KLKB1*, *GPR32*, *ADM*, *NUPR1*, *SCN9A*, *IL17B*, *CX3CL1*, *FFAR3*, *PYDC2*, *SYT11*, *RORA*, and *GPR31*) with high diagnostic efficacy were identified (Figure 2A and B). Nine machine learning algorithms (KNN, RF, LR, SVM, DT, XGBoost, LightGBM, ANN, and CatBoost) were employed to construct diagnostic models based on genes with high diagnostic efficacy. The Support Vector Machine (SVM) exhibited the highest AUC value for the validation set. Consequently, the SVM was selected as the final diagnostic model, and four model genes (*ADM*, *NUPR1*, *PTGER1*, and *PYDC2*), regarded as biomarkers, were screened out (Figure 2C and D). Through Principal Component Analysis (PCA), the expression levels of these four biomarkers in the GSE113079 dataset distinguished the CAD and normal groups (Figure 2E). Among the four biomarkers, NUPR1 exhibited the highest coefficient (Figure 2F). A nomogram was developed to predict disease probability in patients with CAD based on *ADM*, *NUPR1*, *PTGER1*, and *PYDC2* (Figure 3A). The calibration, decision, and clinical impact curves were plotted based on the nomogram, demonstrating the predictive ability of the model was favorable (Figure 3B-D).

Functional Enrichment and miRNA-TF-mRNA Network Analysis

To further investigate the role of the selected biomarkers in inflammatory responses to CAD, GSEA and network analyses were conducted. GO functional enrichment analysis revealed that *ADM*, *NUPR1*, *PTGER1*, and *PYDC2* predominantly participated in the processes of "macroautophagy", "ubiquitin-like protein ligase activity", and "peptide receptor activity". KEGG enrichment analysis indicated that these four biomarkers (*ADM*, *NUPR1*, *PTGER1*, and *PYDC2*) were involved in "cellular senescence", the "TNF signaling pathway", and "linoleic acid metabolism"

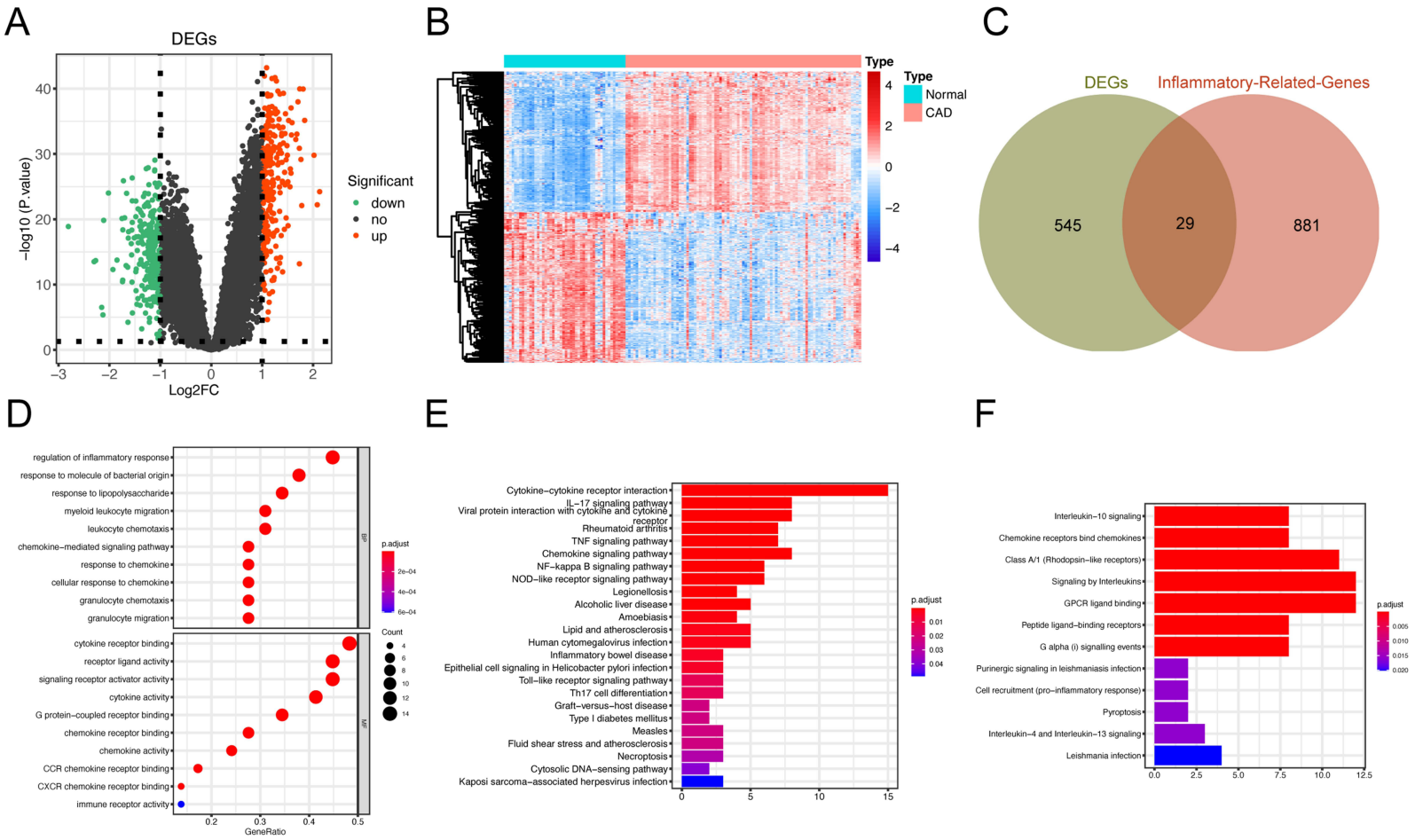

Figure 1 Identification of DEG and DIRGs in CAD. (**A**) Volcano map of DEGs between CAD and normal samples. (**B**) Heatmap of DEGs between CAD and normal samples. (**C**) Venn diagram of the intersection of DEGs and inflammatory related genes. (**D**) GO functional enrichment analysis of DIRGs. (**E**) KEGG functional enrichment analysis of DIRGs. (**F**) REACTOME functional enrichment analysis.

https://doi.org/10.2147/JIR.S496046

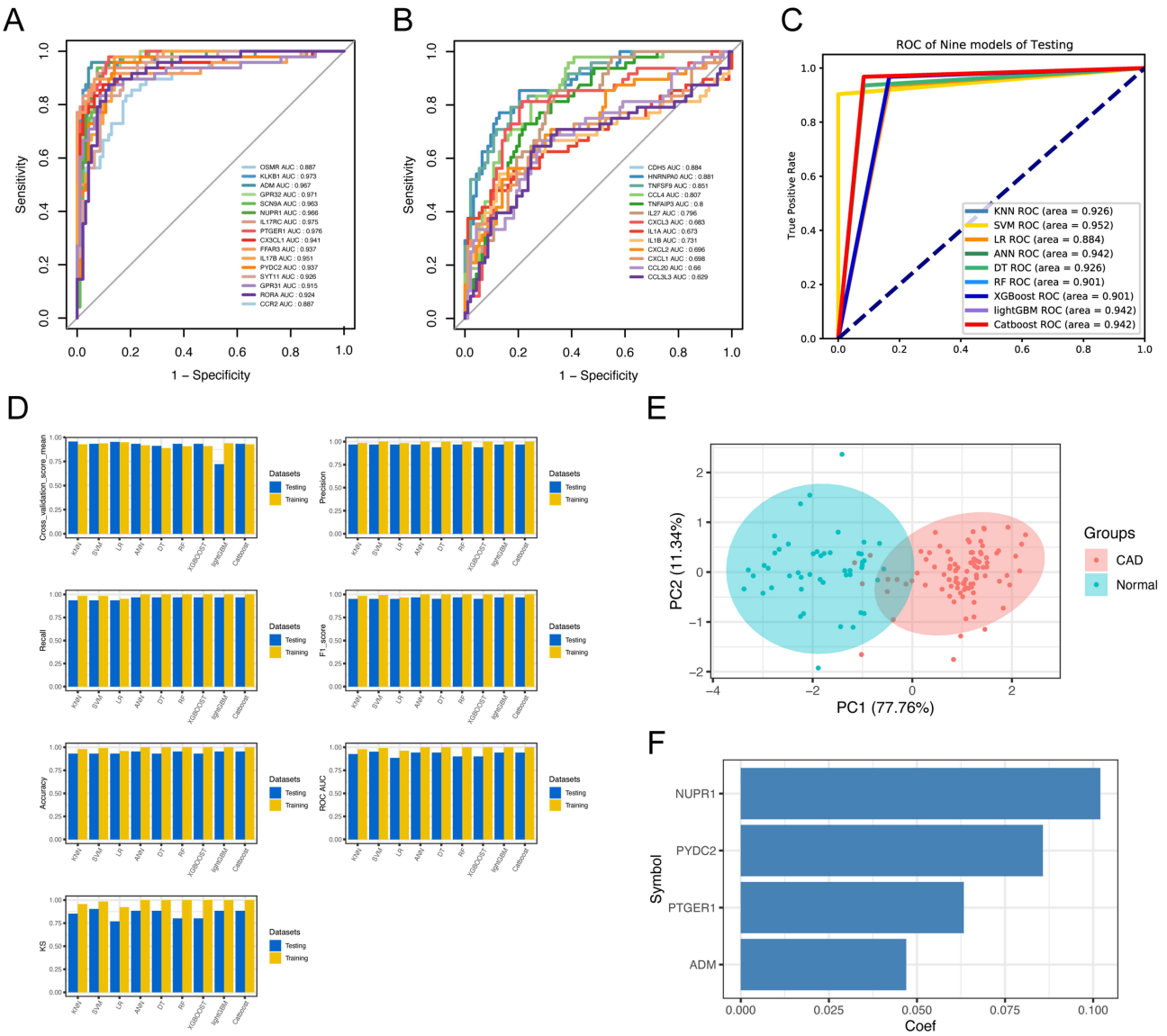

Figure 2 Machine learning in screening candidate diagnostic biomarkers for CAD. (**A-B**). The area under curve (AUC) for candidate biomarkers. (**C**) ROC analysis of diagnostic models constructed by machine algorithms (KNN, RF, LR, SVM, DT, XGBoost, LightGBM, ANN and CatBoost). (**D**) Cross-validation (CV) of diagnostic models constructed by machine algorithms. (**E**) PCA analysis of CAD and normal groups based on the expression levels of *ADM, NUPR1, PTGER1* and *PYDC2*. (**F**) The coefficient of *ADM, NUPR1, PTGER1* and *PYDC2*.

(Figure 4A-B, Supplementary 7–14). Moreover, a total of 1661 miRNA-mRNA regulatory relationship pairs were predicted using the miRWalk database, including 1283 miRNAs, and 66 regulatory relationship pairs of TF-mRNAs were acquired using the AnimalTFDB database, comprising 23 TFs. According to the TransmiR database, 35 regulatory relationship pairs of TF-miRNAs were predicted, encompassing 25 miRNAs and 23 TFs. A total of 212 miRNA-TF regulatory relationships were predicted using the miRWalk database, encompassing 23 TFs and 25 miRNAs. A total of 559 pairs of miRNA-miRNAs were identified as having potential interactions with 51 miRNAs (Figure 4C, Supplementary 15). The predicted TFs have been reported as master regulators of inflammatory activation (*CEBPB, JUN, NFKB1, HIF1A, FOXO3*),[18–22] the cell cycle (*RUNX1, E2F1, RB1)*[23,24] and cellular apoptosis (*MYCN, TP53*).[25,26]

Immune Cell Profile in CAD

The proportion of immune cells was analyzed using the CIBERSORT algorithm, and 22 types of immune cells were identified in both normal and CAD samples (Figure 5A-B). $CD8^+$ T cells, $CD4^+$ memory T cells (activated), and NK cells

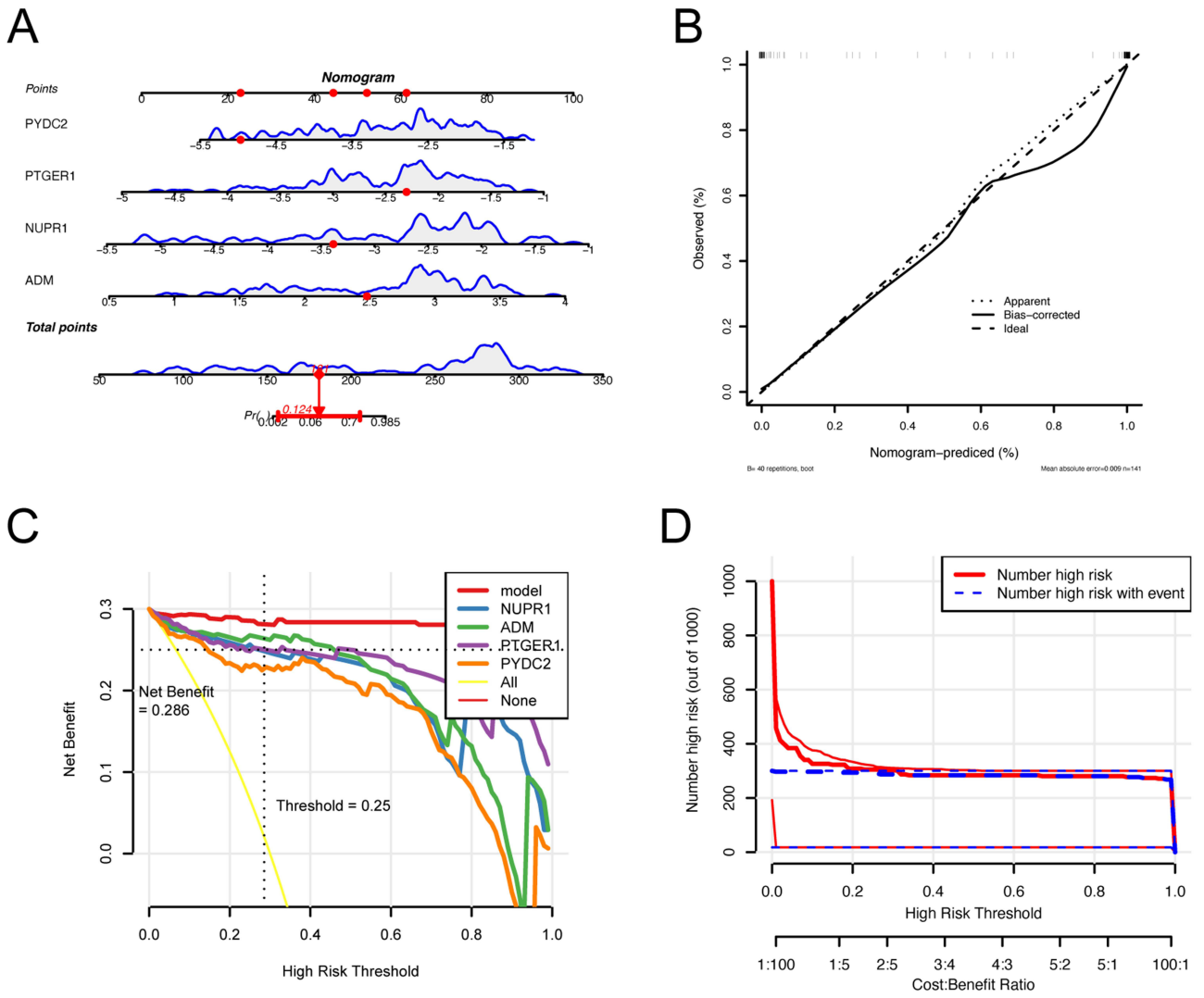

Figure 3 The prediction performance of selected biomarkers. (**A**) nomogram of disease probability prediction in CAD. (**B**) The calibration curve of nomogram. (**C**) The decision curve of diagnostic model. (**D**) The clinical impact curve of diagnostic model.

(resting and activated) were significantly lower in the CAD group, whereas monocyte, regulatory T cells (Tregs) and CD4 naïve T cells were higher than those in the normal group (Figure 5C). According to Pearson correlation analysis, *PYDC2* had the strongest positive correlation with Tregs (R=0.46), while *PTGER1* (R=0.4), *NUPR1* (R=0.54), and *ADM* (R=0.46) exhibited significant positive correlations with monocytes. Furthermore, it was observed that these four biomarkers (*ADM*, *NUPR1*, *PTGER1*, and *PYDC2*) were highly negatively correlated with resting NK cells, with correlation coefficients of −0.4, −0.45, −0.32, and −0.3, respectively (Figure 5D). These results indicate that the selected biomarkers may participate in the regulation of monocyte- and Treg cell-mediated immune responses in CAD.

Validation of Biomarkers

To further validate the expression levels of the four selected biomarkers, PBMCs were isolated from the enrolled CAD patients and age-matched controls. qPCR analyses confirmed the increased mRNA levels of *ADM*, *NUPR1*, *PTGER1* and *PYDC2* in the CAD group (Figure 6A). A mouse atherosclerosis model was established to further investigate the role of these biomarkers in atherosclerotic arteries. ApoE$^{-/-}$ mice fed a high-fat diet exhibited aggravated atherosclerotic lesions compared to those fed a normal chow diet (Figure 6C). As *PYDC2* is not expressed in mice, the mRNA levels of *ADM*, *NUPR1*, and *PTGER1* were analyzed in the mouse aorta. The expression of *ADM*, *NUPR1*, and *PTGER1* was

https://doi.org/10.2147/JIR.S496046

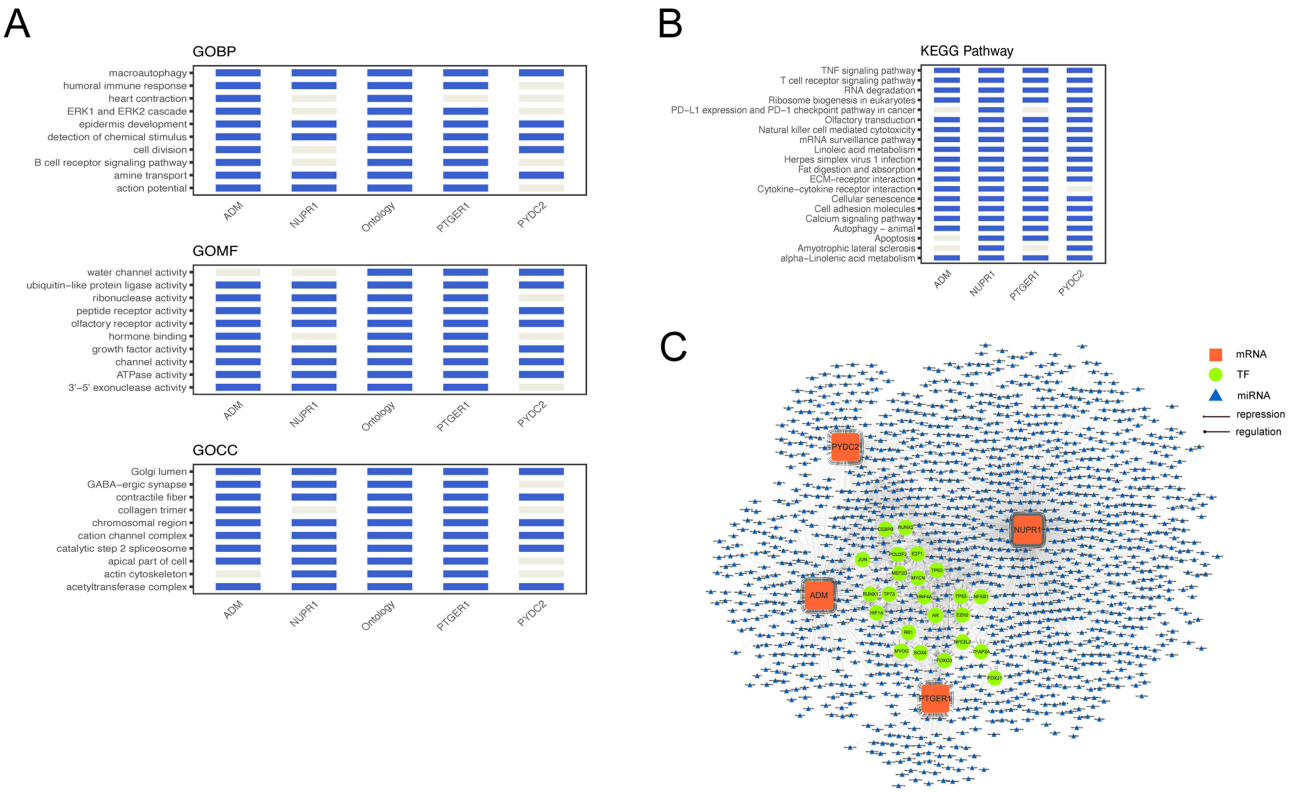

Figure 4 GSEA and miRNA-TF-mRNA network analysis of selected biomarkers. (**A**) GO enrichment analysis of biomarkers. (**B**) KEGG pathway enrichment analysis of biomarkers. (**C**) miRNA-TF-mRNA network analysis of biomarkers.

significantly upregulated in the aorta of the high-fat diet (HFD) group (Figure 6B), which validated the increased levels of these biomarkers in atherosclerotic arteries as well as in PBMCs.

Discussion

CAD diagnosis predominantly depends on angiography, an invasive and costly procedure. This study utilized a comprehensive bioinformatic approach and machine learning algorithms to identify potential diagnostic biomarkers for CAD. Four candidate genes (*ADM*, *NUPR1*, *PTGER1*, and *PYDC2*) were identified, demonstrating diagnostic value for CAD for the first time. Furthermore, the expression levels of these biomarkers were validated in peripheral blood mononuclear cells (PBMCs) from CAD patients and atherosclerotic aortas in mice. Our study demonstrates that the selected biomarkers are closely associated with the pathogenic mechanisms of atherosclerosis, thereby facilitating the development of innovative therapeutic targets.

CAD is a chronic inflammatory disease characterized by inflammatory activation and the recruitment of immune cells to atherosclerotic lesions.[27] GO and KEGG analyses of DIRGs in CAD patients indicated an enrichment in the "Regulation of inflammatory response", "Chemokine-mediated signaling pathway" and "IL-17, TNF, NF-KappaB signaling pathways". These pathways are recognized as key mechanisms underlying the inflammatory activation of CAD, and the identified biomarkers are implicated in these pathways.[28–31] *ADM* (Adrenomedullin) is a vasodilatory peptide with multiple physiological functions, including the maintenance of vascular tone and endothelial barrier function.[32] Evidence suggests that *ADM* levels increase in sepsis and cardiovascular diseases and that *ADM* is considered a biomarker for inflammatory and cardiovascular conditions, including atherosclerosis and heart failure.[33–35] Andrade et al reported that *NUPR1* (Nuclear protein 1) serves as a key regulator of the type I IFN response in monocyte-derived macrophages, suggesting that *NUPR1* may participate in the pro-inflammatory activation of monocytes/macrophages.[36] *PTGER1* (Prostaglandin E receptor 1) is one of the four prostaglandin receptors involved in biological processes, including immunity, inflammation, and blood pressure regulation.[37,38] Notably, we found that the expression of *PTGER1*, *NUPR1*, and *ADM* was significantly positively correlated with monocytes. Furthermore, our animal experimental results demonstrated increased levels of *PTGER1*, *NUPR1*, and *ADM*

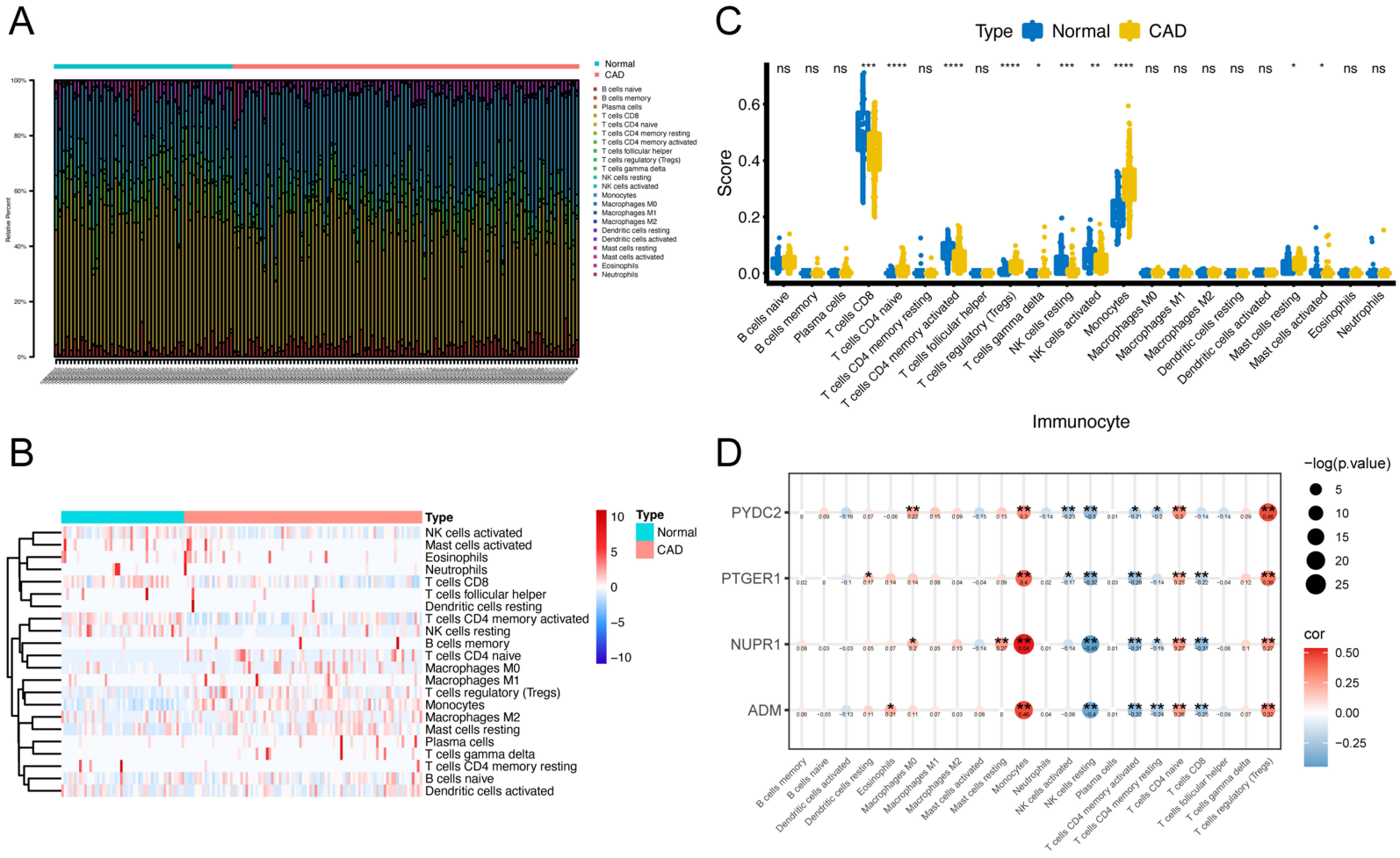

Figure 5 Different immune cell profile between CAD and normal subjects. (**A-B**) The proportion of immune cells was analyzed by CIBERSORT algorithm. (**C**) The difference of immune cell between CAD and normal subjects. (**D**) The correlation of selected biomarker with immune cells. (ns represented $P > 0.05$, not significant; * represented $P < 0.05$; ** represented $P < 0.01$; *** represented $P < 0.001$; ****$P < 0.0001$ between the two group).

https://doi.org/10.2147/JIR.S496046

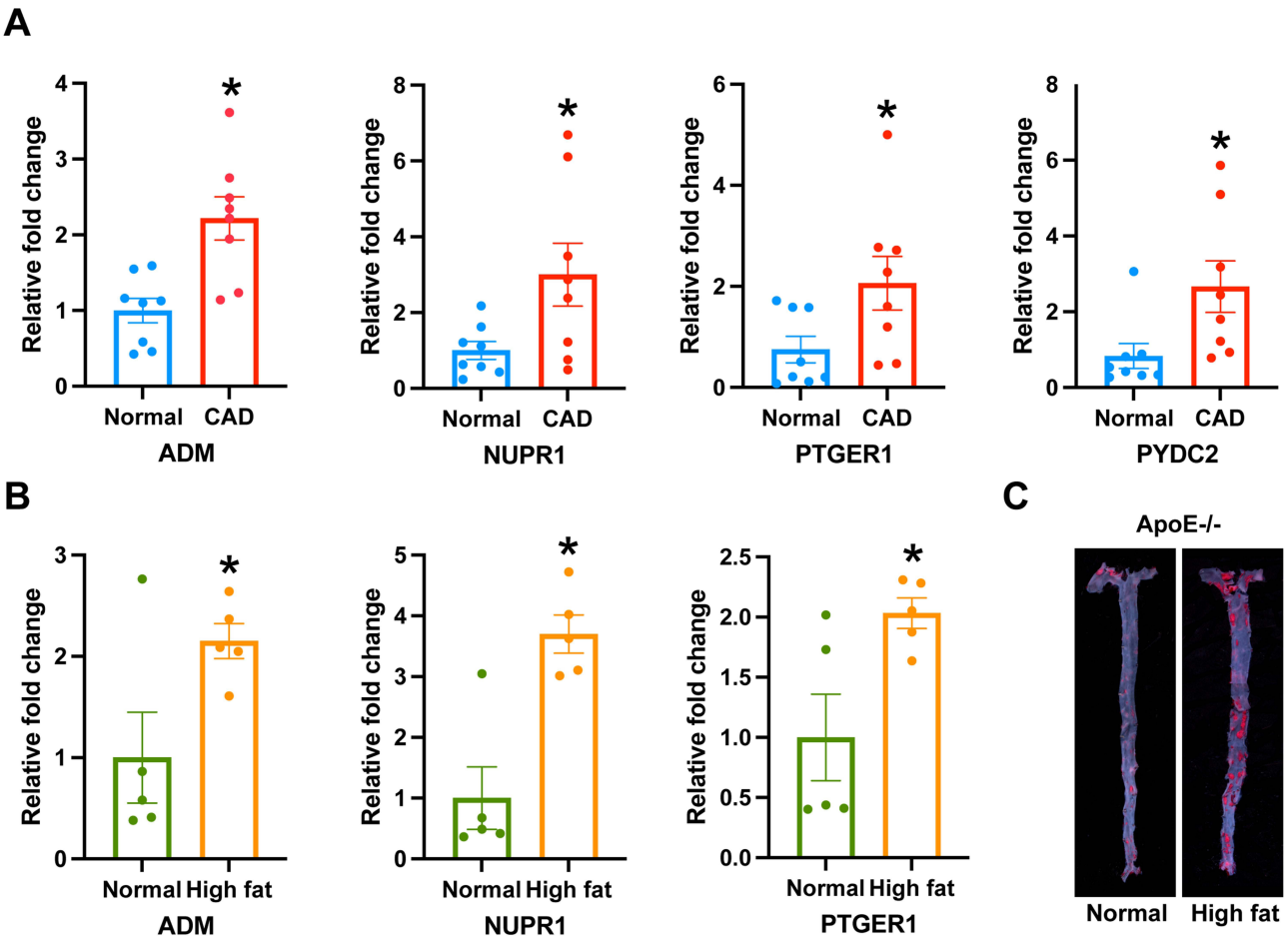

Figure 6 Validation of biomarkers in PBMCs and mouse atherosclerotic aorta. (**A**) mRNA levels of *ADM*, *NUPR1*, *PTGER1* and *PYDC2* in PBMCs from CAD and normal subjects. (**B**) mRNA levels of *ADM*, *NUPR1*, *PTGER1* in aorta from ApoE$^{-/-}$ mice fed with high fat diet or normal chow. (**C**) Representative of aorta from ApoE$^{-/-}$ mice fed with high fat diet or normal chow. (* represented $P < 0.05$ between the two group).

in the atherosclerotic aortas of mice. These findings suggest their potential roles in the development of atherosclerosis, wherein monocyte infiltration is a critical mechanism.

Compared to *PTGER1*, *NUPR1*, and *ADM*, *PYDC2* exhibited the strongest positive correlation with Tregs, which were significantly increased in the peripheral blood of patients with CAD, indicating their important role in the etiology of CAD. Evidence indicates that *PYDC2* inhibits inflammasome assembly by binding to ASC, thereby preventing caspase-1 activation and cytokine release.[39] Tregs play a crucial role in modulating and suppressing inflammatory responses, maintaining immune system equilibrium, and curbing excessive immune reactions. Treg cells hinder the aggregation of pro-inflammatory cells and the subsequent release of associated inflammatory cytokines, both of which are pivotal processes in cardiovascular diseases.[40] Treg cells hinder the aggregation of pro-inflammatory cells and subsequent release of associated inflammatory cytokines, which are pivotal processes in cardiovascular diseases.[41] Given the protective role of *PYDC2* and Treg cells, the increase in *PYDC2* in CAD patients might reflect feedback regulation of the pro-inflammatory states in these patients. Further investigations are required to explore *PYDC2*- and Treg-regulated immune responses in CAD.

Additionally, we observed a highly significant negative correlation between four biomarkers (*ADM*, *NUPR1*, *PTGER1*, and *PYDC2*) and resting NK cells. The rate of spontaneous NK cell apoptosis was elevated in CAD patients.[42,43] Our miRNA-TF-mRNA network analyses predicted that the cell cycle- and apoptosis-regulated TFs may be involved in the modulation of selected biomarkers, indicating the potential role of these biomarkers in mediating immune cell apoptosis.

Overall, our study provides comprehensive insights into the molecular mechanisms and potential biomarkers associated with CAD, offering valuable information for further research and clinical translation. However, further experimental validation is warranted to confirm the functional roles of the identified biomarkers and their potential as

therapeutic targets in CAD management. Additionally, larger longitudinal studies are needed to assess the prognostic value of the identified biomarkers in larger patient cohorts.

Conclusion

In conclusion, we identified the inflammatory gene signature of CAD through bioinformatic approaches and selected *ADM*, *NUPR1*, *PTGER1*, and *PYDC2* as potential CAD biomarkers using machine learning algorithms. Further validations confirmed the elevated levels of the selected biomarkers in PBMCs from CAD patients and in the atherosclerotic aorta from $ApoE^{-/-}$ mice. Our study provides novel inflammatory biomarkers with potential diagnostic value for CAD.

Funding

This work was supported by the National Natural Science Foundation of China (82270429, 82400507, 82270458, and 82470456), Guangdong Basic and Applied Basic Research Foundation (2022A1515012270 and 2021A1515220019), Guangzhou Key-Area R&D Program (202206080004) and China Heart House-Chinese Cardiovascular Association HX fund (2022-CCA-HX-040).

Disclosure

The authors report no conflicts of interest in this work.

References

1. Roth GA, Mensah GA, Johnson CO, et al. Global burden of cardiovascular diseases and risk factors, 1990-2019: update from the GBD 2019 study. *J Am Coll Cardiol*. 2020;76(25):2982–3021. doi:10.1016/j.jacc.2020.11.010
2. Collaborators GBDM. Global, regional, and national under-5 mortality, adult mortality, age-specific mortality, and life expectancy, 1970-2016: a systematic analysis for the global burden of disease study 2016. *Lancet*. 2017;390(10100):1084–1150.
3. Patel MR, Peterson ED, Dai D, et al. Low diagnostic yield of elective coronary angiography. *N Engl J Med*. 2010;362(10):886–895. doi:10.1056/NEJMoa0907272
4. Libby P, Ridker PM, Hansson GK. Progress and challenges in translating the biology of atherosclerosis. *Nature*. 2011;473(7347):317–325. doi:10.1038/nature10146
5. Soehnlein O, Libby P. Targeting inflammation in atherosclerosis - from experimental insights to the clinic. *Nat Rev Drug Discov*. 2021;20(8):589–610. doi:10.1038/s41573-021-00198-1
6. Ridker PM, Everett BM, Pradhan A, et al. Low-dose methotrexate for the prevention of atherosclerotic events. *N Engl J Med*. 2019;380(8):752–762. doi:10.1056/NEJMoa1809798
7. Ridker PM. The time to initiate anti-inflammatory therapy for patients with chronic coronary atherosclerosis has arrived. *Circulation*. 2023;148(14):1071–1073. doi:10.1161/CIRCULATIONAHA.123.066510
8. Nelson K, Fuster V, Ridker PM. Low-dose colchicine for secondary prevention of coronary artery disease: JACC review topic of the week. *J Am Coll Cardiol*. 2023;82(7):648–660. doi:10.1016/j.jacc.2023.05.055
9. Ferencik M, Mayrhofer T, Lu MT, et al. Coronary atherosclerosis, cardiac troponin, and interleukin-6 in patients with chest pain: the PROMISE trial results. *JACC Cardiovasc Imaging*. 2022;15(8):1427–1438. doi:10.1016/j.jcmg.2022.03.016
10. Reel PS, Reel S, Pearson E, Trucco E, Jefferson E. Using machine learning approaches for multi-omics data analysis: a review. *Biotechnol Adv*. 2021;49:107739. doi:10.1016/j.biotechadv.2021.107739
11. Ritchie ME, Phipson B, Wu D, et al. limma powers differential expression analyses for RNA-sequencing and microarray studies. *Nucleic Acids Res*. 2015;43(7):e47. doi:10.1093/nar/gkv007
12. Ito K, Murphy D. Application of ggplot2 to pharmacometric graphics. *CPT Pharmacometrics Syst Pharmacol*. 2013;2(10):e79. doi:10.1038/psp.2013.56
13. Wu T, Hu E, Xu S, et al. clusterProfiler 4.0: a universal enrichment tool for interpreting omics data. *Innovation*. 2021;2(3):100141. doi:10.1016/j.xinn.2021.100141
14. Bo C, Zhang H, Cao Y, et al. Construction of a TF-miRNA-gene feed-forward loop network predicts biomarkers and potential drugs for myasthenia gravis. *Sci Rep*. 2021;11(1):2416. doi:10.1038/s41598-021-81962-6
15. Engelbertsen D, Rattik S, Wigren M, et al. IL-1R and MyD88 signalling in CD4+ T cells promote Th17 immunity and atherosclerosis. *Cardiovasc Res*. 2018;114(1):180–187. doi:10.1093/cvr/cvx196
16. Haghikia A, Zimmermann F, Schumann P, et al. Propionate attenuates atherosclerosis by immune-dependent regulation of intestinal cholesterol metabolism. *Eur Heart J*. 2022;43(6):518–533. doi:10.1093/eurheartj/ehab644
17. Kaur H, Carvalho J, Looso M, et al. Single-cell profiling reveals heterogeneity and functional patterning of GPCR expression in the vascular system. *Nat Commun*. 2017;8(1):15700. doi:10.1038/ncomms15700
18. Perino A, Pols TW, Nomura M, Stein S, Pellicciari R, Schoonjans K. TGR5 reduces macrophage migration through mTOR-induced C/EBPbeta differential translation. *J Clin Invest*. 2014;124(12):5424–5436. doi:10.1172/JCI76289
19. Law C, Wacleche VS, Cao Y, et al. Interferon subverts an AHR-JUN axis to promote CXCL13(+) T cells in lupus. *Nature*. 2024;631(8022):857–866. doi:10.1038/s41586-024-07627-2

20. Zhong Z, Umemura A, Sanchez-Lopez E, et al. NF-kappaB restricts inflammasome activation via elimination of damaged mitochondria. *Cell*. 2016;164(5):896–910. doi:10.1016/j.cell.2015.12.057
21. Shalova IN, Lim JY, Chittezhath M, et al. Human monocytes undergo functional re-programming during sepsis mediated by hypoxia-inducible factor-1alpha. *Immunity*. 2015;42(3):484–498. doi:10.1016/j.immuni.2015.02.001
22. Lee JC, Espeli M, Anderson CA, et al. Human SNP links differential outcomes in inflammatory and infectious disease to a FOXO3-regulated pathway. *Cell*. 2013;155(1):57–69. doi:10.1016/j.cell.2013.08.034
23. Martinez-Soria N, McKenzie L, Draper J, et al. The oncogenic transcription factor RUNX1/ETO corrupts cell cycle regulation to drive leukemic transformation. *Cancer Cell*. 2019;35(4):705. doi:10.1016/j.ccell.2019.03.012
24. Schuldt A. Cell cycle: E2F1 ensures the endocycle. *Nat Rev mol Cell Biol*. 2011;12(12):768. doi:10.1038/nrm3232
25. Ham J, Costa C, Sano R, et al. Exploitation of the apoptosis-primed state of MYCN-amplified neuroblastoma to develop a potent and specific targeted therapy combination. *Cancer Cell*. 2016;29(2):159–172. doi:10.1016/j.ccell.2016.01.002
26. Boon NJ, Oliveira RA, Korner PR, et al. DNA damage induces p53-independent apoptosis through ribosome stalling. *Science*. 2024;384 (6697):785–792. doi:10.1126/science.adh7950
27. Harrington RA. Targeting inflammation in coronary artery disease. *N Engl J Med*. 2017;377(12):1197–1198. doi:10.1056/NEJMe1709904
28. Aukrust P, Halvorsen B, Yndestad A, et al. Chemokines and cardiovascular risk. *Arterioscler Thromb Vasc Biol*. 2008;28(11):1909–1919. doi:10.1161/ATVBAHA.107.161240
29. Potekhina AV, Pylaeva E, Provatorov S, et al. Treg/Th17 balance in stable CAD patients with different stages of coronary atherosclerosis. *Atherosclerosis*. 2015;238(1):17–21. doi:10.1016/j.atherosclerosis.2014.10.088
30. Nash M, McGrath JP, Cartland SP, Patel S, Kavurma MM. Tumour necrosis factor superfamily members in ischaemic vascular diseases. *Cardiovasc Res*. 2019;115(4):713–720. doi:10.1093/cvr/cvz042
31. Monaco C, Paleolog E. Nuclear factor kappaB: a potential therapeutic target in atherosclerosis and thrombosis. *Cardiovasc Res*. 2004;61 (4):671–682. doi:10.1016/j.cardiores.2003.11.038
32. Voors AA, Kremer D, Geven C, et al. Adrenomedullin in heart failure: pathophysiology and therapeutic application. *Eur J Heart Fail*. 2019;21 (2):163–171. doi:10.1002/ejhf.1366
33. Voordes G, Davison B, Biegus J, et al. Biologically active adrenomedullin as a marker for residual congestion and early rehospitalization in patients hospitalized for acute heart failure: data from STRONG-HF. *Eur J Heart Fail*. 2024;26(7):1480–1492. doi:10.1002/ejhf.3336
34. Balint L, Nelson-Maney NP, Tian Y, Serafin SD, Caron KM. Clinical potential of adrenomedullin signaling in the cardiovascular system. *Circ Res*. 2023;132(9):1185–1202. doi:10.1161/CIRCRESAHA.123.321673
35. Hofbauer KH, Schoof E, Kurtz A, Sandner P. Inflammatory cytokines stimulate adrenomedullin expression through nitric oxide-dependent and -independent pathways. *Hypertension*. 2002;39(1):161–167. doi:10.1161/hy1201.097201
36. Ra P, Mehta M, Lu J, et al. The cell fate regulator NUPR1 is induced by Mycobacterium leprae via type I interferon in human leprosy. *PLoS Negl Trop Dis*. 2019;13(7):e0007589. doi:10.1371/journal.pntd.0007589
37. Rutkai I, Feher A, Erdei N, et al. Activation of prostaglandin E2 EP1 receptor increases arteriolar tone and blood pressure in mice with type 2 diabetes. *Cardiovasc Res*. 2009;83(1):148–154. doi:10.1093/cvr/cvp098
38. Caristi S, Piraino G, Cucinotta M, Valenti A, Loddo S, Teti D. Prostaglandin E2 induces interleukin-8 gene transcription by activating C/EBP homologous protein in human T lymphocytes. *J Biol Chem*. 2005;280(15):14433–14442. doi:10.1074/jbc.M410725200
39. Ratsimandresey RA, Chu LH, Khare S, et al. The PYRIN domain-only protein POP2 inhibits inflammasome priming and activation. *Nat Commun*. 2017;8(1):15556. doi:10.1038/ncomms15556
40. Chaudhry A, Rudensky AY. Control of inflammation by integration of environmental cues by regulatory T cells. *J Clin Invest*. 2013;123 (3):939–944. doi:10.1172/JCI57175
41. Foks AC, Lichtman AH, Kuiper J. Treating atherosclerosis with regulatory T cells. *Arterioscler Thromb Vasc Biol*. 2015;35(2):280–287. doi:10.1161/ATVBAHA.114.303568
42. Li W, Lidebjer C, Yuan XM, et al. NK cell apoptosis in coronary artery disease: relation to oxidative stress. *Atherosclerosis*. 2008;199(1):65–72. doi:10.1016/j.atherosclerosis.2007.10.031
43. Szymanowski A, Li W, Lundberg A, et al. Soluble Fas ligand is associated with natural killer cell dynamics in coronary artery disease. *Atherosclerosis*. 2014;233(2):616–622. doi:10.1016/j.atherosclerosis.2014.01.030